Harmonic analysis of grid-connected parallel H-bridge VSI and CSI with isolated DC sources

Suroso, Winasis, Priswanto
Department of Electrical Engineering, Faculty of Engineering, Jenderal Soedirman University, Purbalingga, Indonesia

Article Info

Article history:

Received Sep 19, 2025
Revised Feb 26, 2026
Accepted Mar 6, 2026

Keywords:

Harmonics
Inverter
Parallel
Power conversion
Power grid

ABSTRACT

In a single-phase inverter system, parallel operation of inverters is a strategy to increase capacity, improve reliability, and increase the flexibility of the inverter system. This work discusses the basic operation of a novel parallel H-bridge current source inverter (H-BCSI) and H-bridge voltage source inverter (H-BVSI) operated in a grid-connected operation with isolated direct current (DC) sources equipped with power transformers. Each inverter circuit employed an independent current controller to regulate its alternating current (AC) output current. The proposed inverter system was tested for different operation conditions, and its characteristics were analyzed, especially for its harmonic profile. The test results showed that if the magnitude of the H-BCSI current was varied, while the H-BVSI current was kept constant, the total harmonic distortion (THD) value of load current was much lower than the THD values of H-BVSI current, H-BCSI current, and grid current, i.e., THD $I_{load} \leq 1\%$. This condition also occurred when the output current of the H-BVSI was increased gradually while the output current of H-BCSI was maintained constant. Moreover, a similar result was also obtained when both inverters' output currents were varied simultaneously with the same value. The test results confirmed that the injected AC current of both inverters during parallel grid-connected operation worked well at unity power factor, and met the standards IEEE 1547 and IEC 61727, of which current THDs were $\leq 5\%$. The proposed grid-connected parallel inverter system worked, supplying a sinusoidal AC load current with high power quality.

Corresponding Author:

Suroso
Department of Electrical Engineering, Faculty of Engineering, Jenderal Soedirman University
Mayjen Sungkono St. Km. 5, Blater, Purbalingga, Central Java 53371, Indonesia
Email: suroso.te@unsoed.ac.id

1. INTRODUCTION

Currently, power electronics converters play a vital role in developing a higher efficiency of renewable energy conversion systems, such as wind power, photovoltaics, and fuel cells [1]-[3]. Power electronics converters become the key technology to realize a modern power grid. Connecting renewable energy sources and distributed power generation into modern power grids has increased the demand for high-performance power converters, such as inverter technologies. In grid-connected applications, inverters not only transform direct current (DC) power to alternating current (AC) but also do a crucial duty in ensuring power quality, system stability, and compliance with international standards such as IEC 61727 and IEEE 1547 [4]-[8]. Among various single-phase inverter topologies, H-BVSIs and H-BCSIs have gained significant attention owing to their distinct operational characteristics and suitability for different applications [9]-[12].

Parallel operation of inverters is a strategy to enhance system scalability, increase power capacity, improve reliability, and facilitate maintenance of the inverter system [13]-[15]. However, the interaction between multiple inverters operating in parallel introduces challenges related to synchronization, load sharing, and power quality, particularly in terms of harmonic distortion [16]-[19]. In conventional parallel voltage source inverters, harmonics in parallel grid-tied inverters are a tricky problem. Multiple inverters feeding the same point of common coupling (PCC) can interact in ways that worsen distortion instead of reducing it [20]-[22]. In case of a parallel inverter with a single DC source, unwanted reactive circulating currents flow between inverters instead of to the load, causing extra heating, possible overcurrent trips, increased losses, and reduced efficiency [23]-[28].

In low and medium-power applications, single-phase inverters are widely employed, such as for residential photovoltaic power generation as stand-alone or grid-connected operation [29], [30]. The H-bridge current source inverter (CSI) offers several advantages when used for grid-connected inverter operation, particularly in renewable energy systems (like photovoltaic systems). The CSI naturally outputs controlled current, which aligns well with grid requirements, as grid codes often prioritize current control over voltage control. It is easier to synchronize with the grid by injecting controlled current waveforms, making the grid connection and operation smoother. Unlike voltage source inverters (VSIs), CSIs inherently prevent high inrush currents, enhancing protection during grid disturbances. Moreover, since the current is inherently limited by the DC-side inductor, CSIs are less prone to damage from grid faults (e.g., short circuits) [31]-[34].

Transformers are often employed in grid-connected inverter systems to provide galvanic isolation, voltage level matching, and mitigation of circulating currents. A galvanic isolation transformer works to enhance safety by preventing DC current flow into the AC grid, reducing shock hazards to maintenance personnel, and preventing potential ground loop currents. When combined with appropriate control strategies, transformers also enable effective decoupling and coordination of inverter operation, thereby impacting the overall power quality at the point of common coupling (PCC). It also provides inherent filtering due to transformer inductance and impedance [35]-[38].

Authors have investigated principal characteristics of single-phase CSI, and VSI operated in parallel as presented in [39]. However, in the previous research, we have not examined the inverter system during grid-connected operation. Based on the author's literature study, there is no literature that has discussed the operation of dissimilar inverter topologies, especially parallel H-BVSI and H-BCSI in grid-connected operation. The problems and operational characteristics of these inverter systems have not been studied well. This paper presents a novel grid-connected parallel H-bridge VSI and H-bridge CSI system using transformer-based interface and with isolated DC power sources. The study investigates the harmonic performance, current sharing, and dynamic response of the inverter system under different operating conditions. Computer simulation-based evaluations were conducted to highlight the advantages of the proposed system and to assess its compliance with IEEE and IEC power quality standards of AC current THD.

2. PROPOSED INVERTER SYSTEM

Figure 1 presents a configuration of two photovoltaic systems connected to the AC power grid using two different inverter circuits via power transformers. This configuration depicts a simplified parallel two-inverter circuit in a grid-tied operation with photovoltaic systems as isolated DC power sources. In reality, more different power inverter circuits can be operated in parallel to serve a common AC power load together with an AC power utility. Figure 2 is a more detailed figure of the proposed inverter system. An H-BVSI and an H-BCSI work in parallel as grid-connected inverters. The H-BCSI is connected to the AC grid using power transformer 2 and filter capacitor C_f. While the H-BVSI employs transformer 1 and inductor filter L_f. The H-BVSI circuits are composed of power switches G_1, G_2, G_3, and G_4. While the H-BCSI circuit is made up of power switches M_1, M_2, M_3, and M_4 in series with diodes to perform unidirectional current. Two different isolated DC power sources are employed for each inverter circuit, as V_{dc1} and V_{dc2}. As can be observed in this figure, the H-BCSI was equipped with a DC current generation circuit composed of power switch Q_{dc}, diode D_F, and power inductor L [39]. In this configuration, the AC power load was supplied by H-BCSI, H-BVSI, and the AC power grid connected at the AC bus.

In order to adjust the power and AC current supplied by two inverter circuits, each inverter was equipped with independent current control circuits. Figure 3 shows the current control and modulation method of the H-BVSI. An AC current sensor S_1 was employed to measure the AC output current of the inverter circuits. The sensor's output signal will be the feedback of the current controller to generate an error signal compared to the current command I_{ref1}. The error signal will be processed by the PI current controller. The output signal of the PI regulator was modulated by two triangular signal carriers in two different circuits of comparators 1 and 2. The AC grid voltage feedback signal obtained by sensing the grid voltage (V_{grid}) with scaling factor α will give synchronization between the injected current by inverters and the power grid voltage.

Moreover, Figure 4 shows the current controller of DC current flowing through the input inductor L of the H-bridge CSI. A PI current controller was also applied in this circuit. However, in this controller, the triangular carrier signal was not implemented. The negative input terminal of the comparator was grounded. Hence, it will make the controller simpler. The output control signal will regulate the operation of switch Q_{dc} to control the magnitude of DC input current I_L. The modulation strategy of H-BCSI is shown in Figure 5. It employed two triangular signals to modulate the sinusoidal reference signal to generate a PWM gating signal from the comparator circuits. The sinusoidal reference signal was generated by sensing the grid voltage that will synchronize both inverters and the AC power grid.

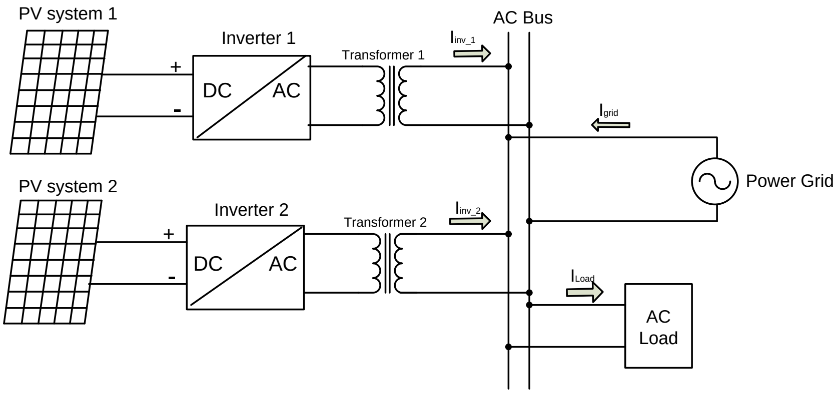

Figure 1. Grid-connected parallel two inverters for PV systems

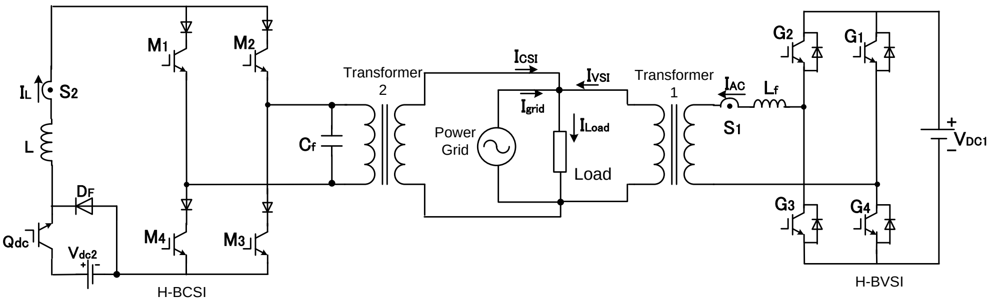

Figure 2. Parallel H-BVSI and H-BCSI for grid-connected operation with transformers

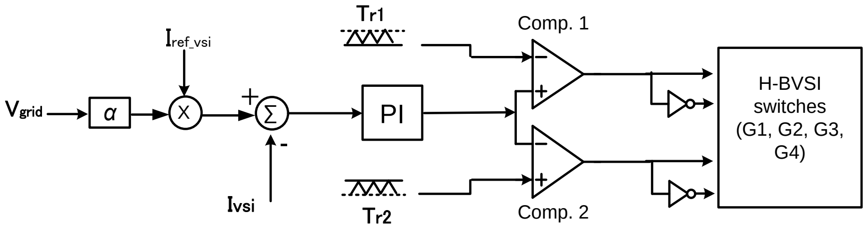

Figure 3. Current controller and PWM modulation of H-BVSI

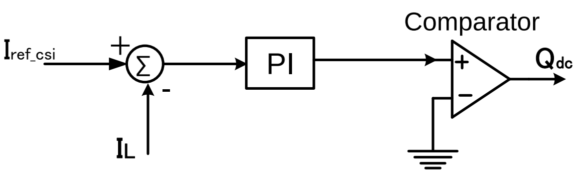

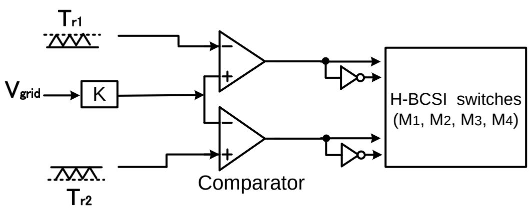

Figure 4. Current controller of H-BCSI [39]

Figure 5. Modulating strategy of H-BCSI [39]

3. TEST RESULTS AND DISCUSSION

In order to investigate the basic characteristics of the proposed grid-connected parallel inverter system, some computer simulation experiments were conducted. Table 1 lists parameters of the tested H-BVSI circuits. The voltage of DC power was set at 24 V. Power MOSFET switches were operated at 21 kHz as the switching frequency to minimize harmonic distortion, and enable a small size of output filter. The fundamental frequency of AC was 50 Hz. The H-bridge VSI inverter was connected to a power transformer 1 via an inductor filter 1 mH. The winding ratio of the transformer was 1:14 to meet the power grid voltage level.

Moreover, Table 2 presents the circuit parameters of the H-BCSI. In this circuit, the DC current source of the inverter circuit was generated by connecting a DC voltage of 24 V to the DC current generation circuit with an inductor of 1 mH. The switching and the main fundamental frequency of inverter operation were 21 kHz and 50 Hz, respectively. The switching speed was the same as that of the H-BVSI. To synchronize the H-BVSI and H-BCSI, the sinusoidal modulating signal was set to the same. The ratio of transformer 2 was also the same as 1: 14. These two inverters were connected to the AC power grid 220 V 50 Hz, worked together supplying power to a resistor R = 100 Ω, and an inductor L = 5 mH connected in series.

Figure 6 shows the measured waveforms of load current (I_{load}), H-BVSI current (I_{vsi}), H-BCSI current (I_{csi}), and grid current (I_{grid}) during parallel grid-connected operation. Both inverters injected sinusoidal currents to the power grid with small distortion and power factor operation at 1. The THD levels of these currents were 0.0094%, 0.34%, 1.64%, and 2.07% for I_{load}, I_{vsi}, I_{csi}, and I_{grid}, respectively. Figure 7 presents the low-order harmonics profile of the load current waveform. All harmonic orders were less than 0.001% of 50 Hz fundamental component. The low harmonics spectrum of the H-BCSI, H-BVSI, and grid currents is described in Figures 8-10, respectively. Small magnitudes of low order harmonics components were confirmed. Moreover, the voltage waveforms of grid voltage (V_{grid}), primary voltage of CSI (V_{pcsi}), and primary voltage of VSI (V_{pvsi}) are shown in Figure 11. Low-distortion sinusoidal voltage waveforms were validated.

Furthermore, Figure 12 presents the transient waveforms of DC inductor current (I_{Lcsi}), secondary current (I_{csi}), and primary current (I_{csi_p}) waveforms of H-bridge CSI, and grid current (I_{grid}) during output current change of H-bridge CSI. Stable DC input current and AC output current of the inverter were achieved by using the applied PI current controller. Test results during a short circuit fault at the power grid were presented in Figure 13. As can be observed, the AC current supplied by both inverters was limited by the current controller command. However, the inverter current did not flow into the power load. The current flowed into the short-circuit point.

Table 1. Test parameters of H-BVSI

Parameters	Value
Input voltage	24 V
Switching frequency	21 kHz
Main output frequency	50 Hz
Transformer ratio	1: 14
Inductor filter	1 mH
AC power grid	220 V, 50 Hz
Load	R = 100 Ω, L= 5 mH

Table 2. Test parameters of H-BCSI

Parameters	Value
DC input voltage	24 V
Input inductor	1 mH
Switching frequency	21 kHz
Main output frequency	50 Hz
Transformer ratio	1: 14
Capacitor filter	10 µF
AC power grid	220 V, 50 Hz
Power load	R =100 Ω, L= 5 mH

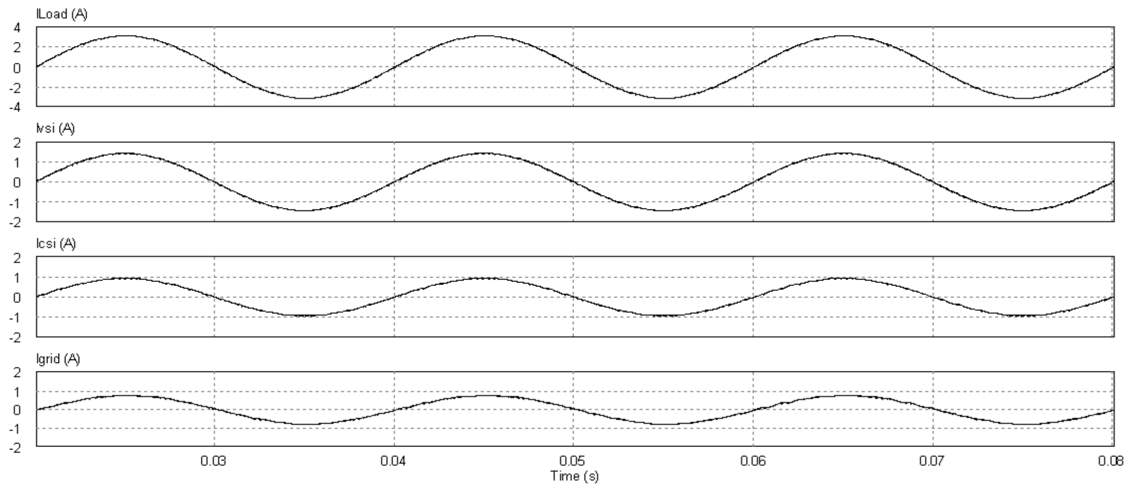

Figure 6. Load current (I_{load}), H-BVSI current (I_{vsi}), H-BCSI current (I_{csi}), and grid current (I_{grid}) waveforms

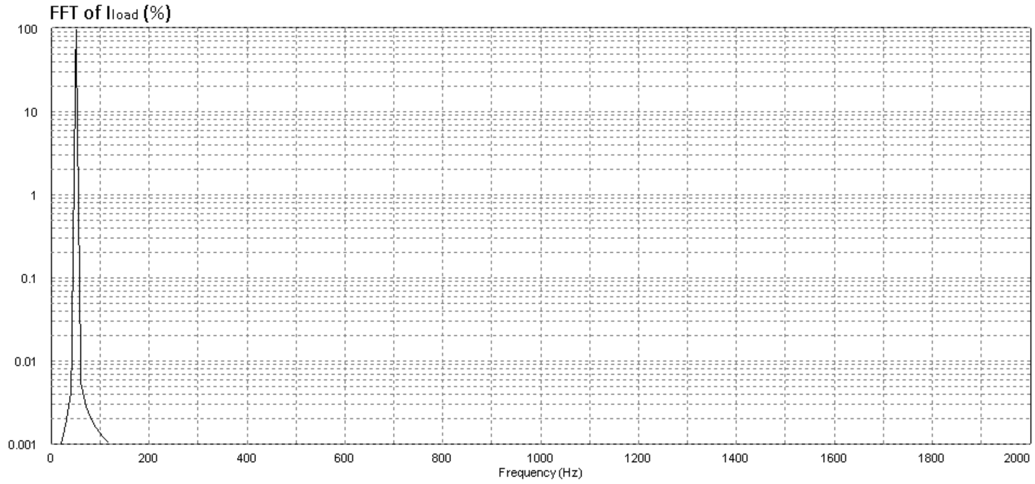

Figure 7. Harmonic analysis result of load current (I_{load})

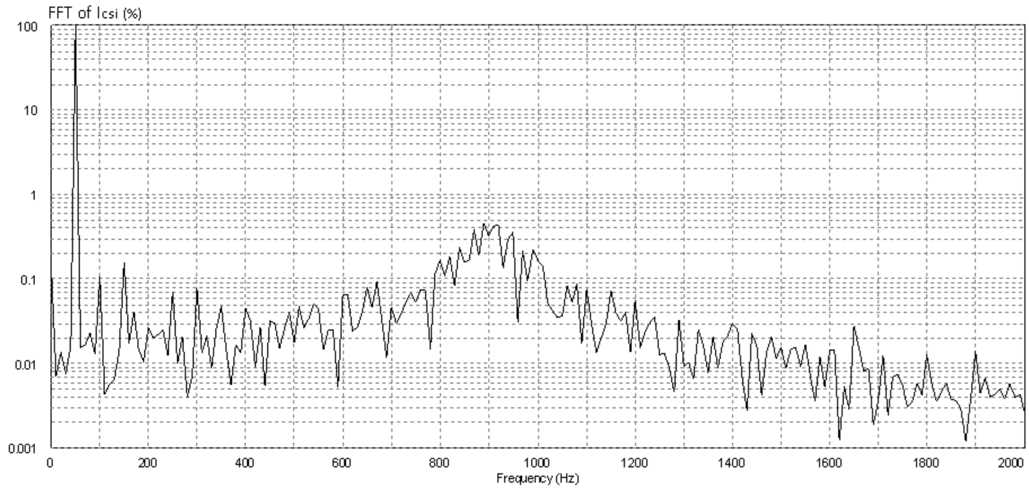

Figure 8. Harmonic analysis result of H-BCSI current (I_{csi})

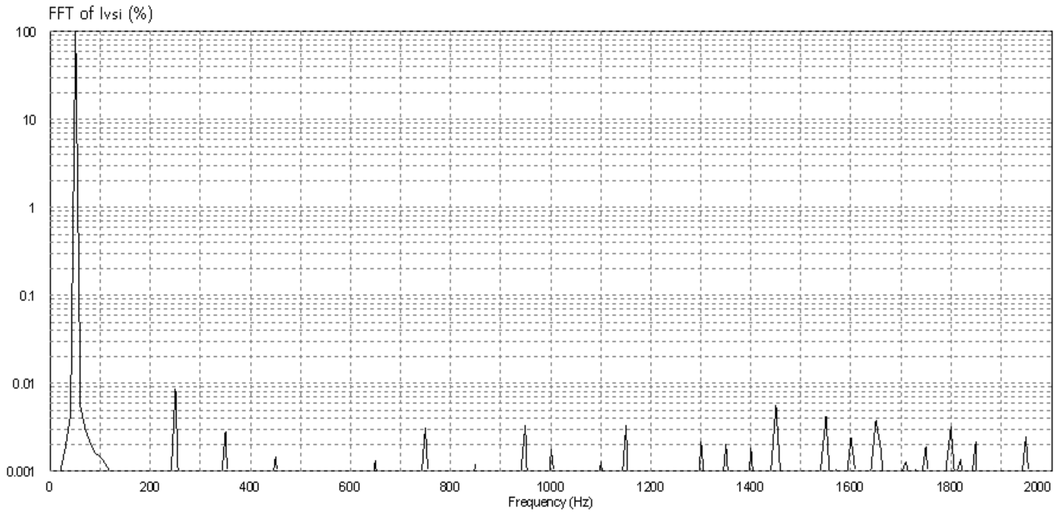

Figure 9. Harmonic analysis result of H-BVSI current (I_{vsi})

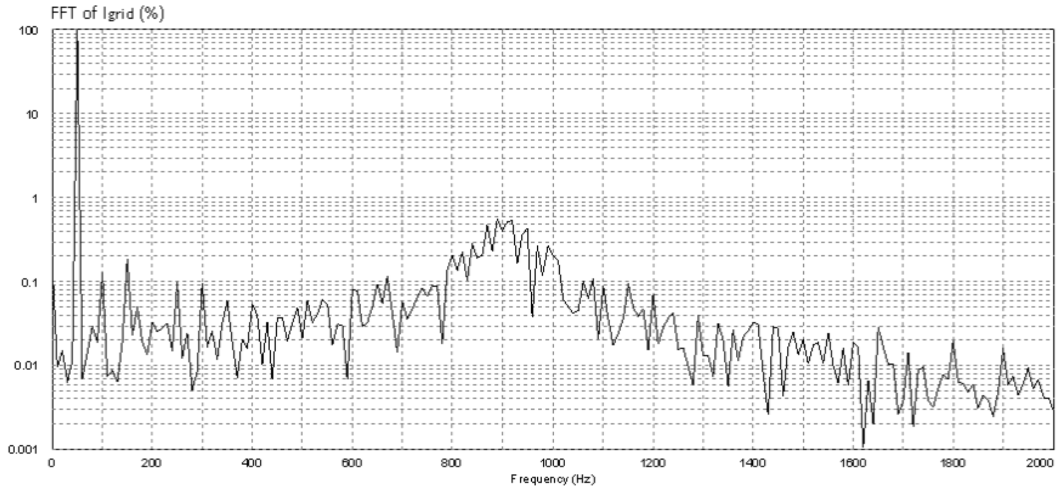

Figure 10. Harmonics profile of grid current (I_{grid})

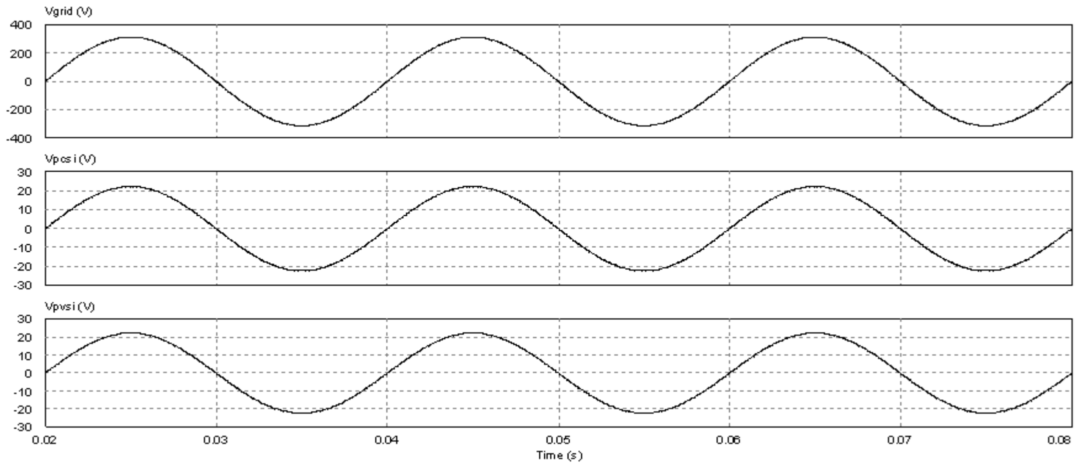

Figure 11. Grid voltage (V_{grid}), primary voltage of CSI (V_{pcsi}), and primary voltage of VSI (V_{pvsi})

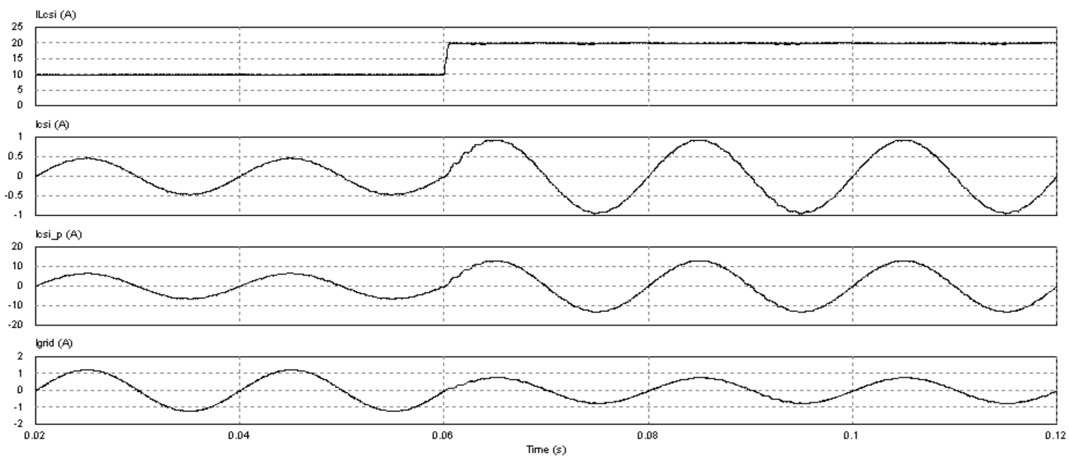

Figure 12. Transient waveforms of DC inductor current (IL_{csi}), secondary current (I_{csi}), and primary current (I_{csi_p}) of H-bridge CSI, and grid current (I_{grid}) waveforms

Figure 14 shows the THD characteristics of I_{vsi}, I_{csi}, I_{load}, and I_{grid} when the magnitude of H-BCSI current (I_{csi}) was varied while the H-BVSI current (I_{vsi}) was kept constant. The THD value of load current (I_{load}) did not improve, even the distortion of I_{vsi} and I_{grid} increased. A small distortion of the load current can be obtained by the proposed parallel operation. This condition was also confirmed when the magnitude of H-bridge VSI current (I_{vsi}) was changed while the H-BCSI current (I_{csi}) was kept constant, as shown in Figure 15. Figure 16 shows THD characteristics of I_{vsi}, I_{csi}, I_{load}, and I_{grid} if the magnitude of H-BVSI current (I_{vsi}) and H-BCSI current (I_{csi}) were increased simultaneously by the same value. The test results of these different conditions have confirmed that a low distortion of the load current waveform was obtained in the proposed parallel grid-connected inverter system. The THD values of the load current, H-BVSI current, and H-BCSI current were <5%.

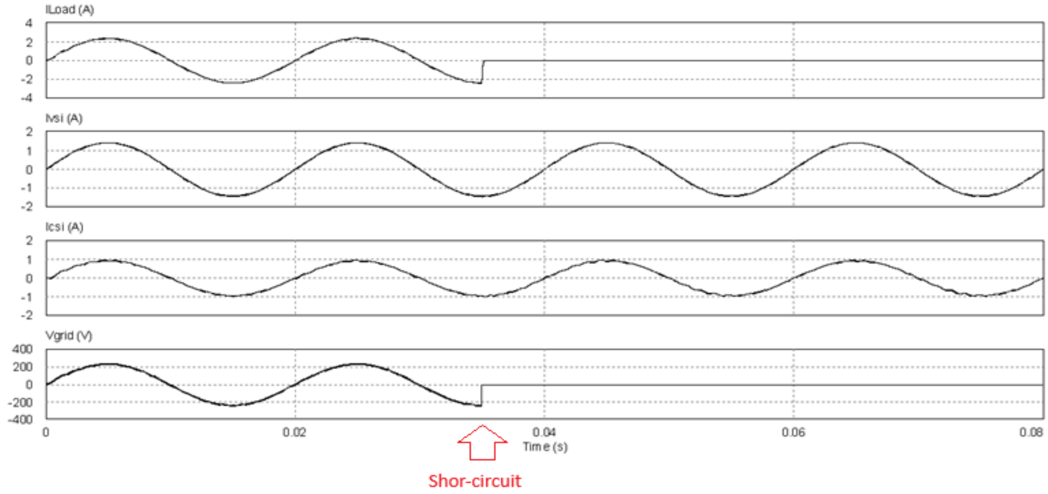

Figure 13. Current and voltage waveforms of I_{load}, I_{vsi}, I_{csi}, and V_{grid} during short circuit fault

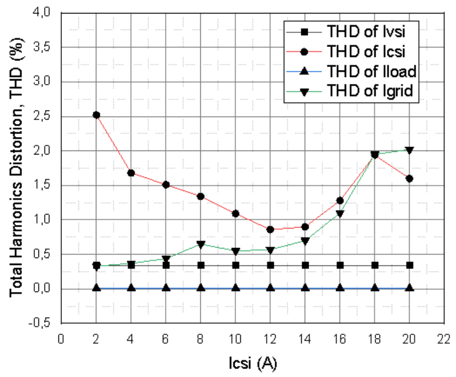

Figure 14. THD characteristics of I_{vsi}, I_{csi}, I_{load}, and I_{grid} when the I_{csi} was varied while I_{vsi} was constant

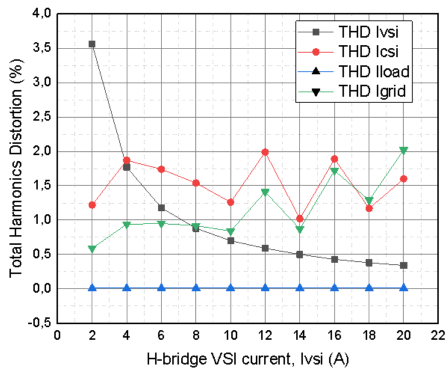

Figure 15. THD characteristics of I_{vsi}, I_{csi}, I_{load}, and I_{grid} when the I_{vsi} was varied while I_{csi} was constant

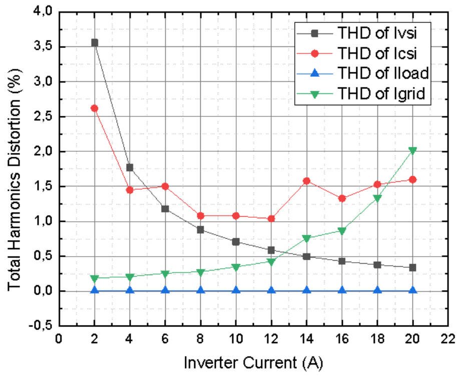

Figure 16. THD characteristics of I_{vsi}, I_{csi}, I_{load}, and I_{grid} when I_{vsi} and I_{csi} were varied by the same value

Figure 17 presents the efficiency profile of the inverter system. Figure 17(a) is the efficiency chart of the H-BVSI. The maximum efficiency was achieved at 98.51%. Figure 17(b) is the efficiency characteristic of H-BCSI with a maximum efficiency 83.4%. The efficiency of H-BCSI was lower than that of H-BVSI. It was caused by additional power losses in the diodes, inductor, and DC generator circuits of the H-BCSI.

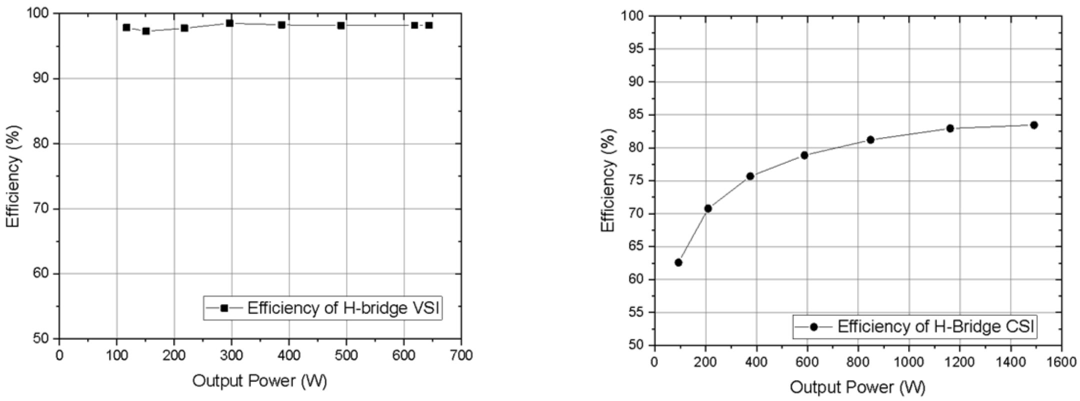

(a) (b)

Figure 17. Efficiency profile of inverter circuit: (a) efficiency of H-BVSI and (b) efficiency of H-BCSI

4. CONCLUSION

A novel operation of H-BVSI and H-BCSI connected to the AC power grid in parallel, and its basic characteristics have been presented and discussed in this paper. The inverters were linked to the AC power grid via a power transformer to meet the voltage level and to attain galvanic isolation between the power inverter and the AC grid. By varying the output current of the two inverters, it has been confirmed that the distortion of load current was much lower than the THD values of the inverters' output currents and grid current. This is a new feature of the proposed parallel inverter system. Furthermore, the inverter system worked well, injecting sinusoidal AC currents to the power grid with high power factor operation and THD value < 5%. The applied current controller worked well, keeping stable DC input current and AC output current of the inverter with low ripples.

FUNDING INFORMATION

This work was funded by a research grant provided by the Regular Fundamental Research Scheme, Directorate General of Higher Education, Ministry of Higher Education, Science, and Technology, Indonesia, in 2025 with contract number 10.77/UN23.34/PT.01.00/VI/2025.

AUTHOR CONTRIBUTIONS STATEMENT

This journal uses the Contributor Roles Taxonomy (CRediT) to recognize individual author contributions, reduce authorship disputes, and facilitate collaboration.

Name of Author	C	M	So	Va	Fo	I	R	D	O	E	Vi	Su	P	Fu
Suroso	✓	✓	✓	✓	✓	✓	✓	✓	✓	✓	✓	✓	✓	✓
Winasis				✓	✓		✓			✓				
Priswanto					✓		✓			✓				

C : **C**onceptualization
M : **M**ethodology
So : **So**ftware
Va : **Va**lidation
Fo : **Fo**rmal analysis
I : **I**nvestigation
R : **R**esources
D : **D**ata Curation
O : Writing - **O**riginal Draft
E : Writing - Review & **E**diting
Vi : **Vi**sualization
Su : **Su**pervision
P : **P**roject administration
Fu : **Fu**nding acquisition

CONFLICT OF INTEREST STATEMENT

Authors state no conflict of interest.

DATA AVAILABILITY

The data that support the findings of this study are available from the corresponding author, [S], upon reasonable request.

REFERENCES

[1] A. Tuluhong, Z. Xu, Q. Chang, and T. Song, "Recent developments in bidirectional DC-DC converter topologies, control strategies, and applications in photovoltaic power generation systems: a comparative review and analysis," *Electronics*, vol. 14, no. 2, p. 389, Jan. 2025, doi: 10.3390/electronics14020389.

[2] P. Catalán, Y. Wang, J. Arza, and Z. Chen, "A comprehensive overview of power converter applied in high-power wind turbine: key challenges and potential solutions," *IEEE Transactions on Power Electronics*, vol. 38, no. 5, pp. 6169–6195, May 2023, doi: 10.1109/TPEL.2023.3234221.

[3] S. Kumar, S. Jammeh, R. Samb, and A. Singh, "Efficient DC–DC power converters for fuel-cell electric vehicle: a qualitative assessment," *IET Power Electronics*, vol. 17, no. 16, pp. 3166–3204, Dec. 2024, doi: 10.1049/pel2.12819.

[4] J. Jana, H. Saha, and K. D. Bhattacharya, "A review of inverter topologies for single-phase grid-connected photovoltaic systems," *Renewable and Sustainable Energy Reviews*, vol. 72, pp. 1256–1270, May 2017, doi: 10.1016/j.rser.2016.10.049.

[5] Y. Zhang, T. Ma, and H. Yang, "Grid-connected photovoltaic battery systems: a comprehensive review and perspectives," *Applied Energy*, vol. 328, p. 120182, Dec. 2022, doi: 10.1016/j.apenergy.2022.120182.

[6] J. Wang, K. Sun, H. Wu, L. Zhang, J. Zhu, and Y. Xing, "Quasi-two-stage multifunctional photovoltaic inverter with power quality control and enhanced conversion efficiency," *IEEE Transactions on Power Electronics*, vol. 35, no. 7, pp. 7073–7085, Jul. 2020, doi: 10.1109/TPEL.2019.2956940.

[7] Z. Xiang *et al.*, "A residential Miniboost photovoltaic inverter with maximum power point operation and power quality compensation," *IEEE Transactions on Industrial Electronics*, vol. 70, no. 5, pp. 4320–4331, May 2023, doi: 10.1109/TIE.2022.3187573.

[8] K. Alluhaybi, I. Batarseh, and H. Hu, "Comprehensive review and comparison of single-phase grid-tied photovoltaic microinverters," *IEEE Journal of Emerging and Selected Topics in Power Electronics*, vol. 8, no. 2, pp. 1310–1329, 2020, doi: 10.1109/JESTPE.2019.2900413.

[9] M. Kumar, "Open circuit fault detection and switch identification for LS-PWM H-bridge inverter," *IEEE Transactions on Circuits and Systems II: Express Briefs*, vol. 68, no. 4, pp. 1363–1367, Apr. 2021, doi: 10.1109/TCSII.2020.3035241.

[10] A. Xin, B. Zhang, C. Zhu, L. Huang, Z. Fang, and Y. Liu, "Design of a high-frequency irreversible electroporation bipolar pulse generator based on H-bridge inverter with an isolating transformer," *IEEE Transactions on Applied Superconductivity*, vol. 34, no. 8, pp. 1–5, Nov. 2024, doi: 10.1109/TASC.2024.3441607.

[11] N. H. Charan, A. Bandyopadhyay, P. Roy, M. A. Babita, and P. M S, "A single-phase cascaded h-bridge multilevel inverter with voltage boost ability: modulation and analysis," *IEEE Transactions on Industry Applications*, vol. 60, no. 3, pp. 3978–3988, May 2024, doi: 10.1109/TIA.2024.3351796.

[12] P. K. Behera, A. Satpathy, and M. Pattnaik, "Design and implementation of a single-band hysteresis current controlled H-bridge inverter," in *2020 3rd International Conference on Energy, Power and Environment: Towards Clean Energy Technologies*, Mar. 2021, pp. 1–6. doi: 10.1109/ICEPE50861.2021.9404454.

[13] A. Sinha and K. Chandra Jana, "Comprehensive review on control strategies of parallel-interfaced voltage source inverters for distributed power generation system," *IET Renewable Power Generation*, vol. 14, no. 13, pp. 2297–2314, Oct. 2020, doi: 10.1049/iet-rpg.2019.1067.

[14] C. Song, R. Zhao, M. Zhu, and Z. Zeng, "Operation method for parallel inverter system with common dc link," *IET Power Electronics*, vol. 7, no. 5, pp. 1138–1147, May 2014, doi: 10.1049/iet-pel.2013.0411.

[15] J. He and Y. W. Li, "An enhanced microgrid load demand sharing strategy," *IEEE Transactions on Power Electronics*, vol. 27, no. 9, pp. 3984–3995, Sep. 2012, doi: 10.1109/TPEL.2012.2190099.

[16] A. Mohd, E. Ortjohann, D. Morton, and O. Omari, "Review of control techniques for inverters parallel operation," *Electric Power Systems Research*, vol. 80, no. 12, pp. 1477–1487, Dec. 2010, doi: 10.1016/j.epsr.2010.06.009.

[17] Z. Liu, J. Liu, X. Hou, Q. Dou, D. Xue, and T. Liu, "Output impedance modeling and stability prediction of three-phase paralleled inverters with master-slave sharing scheme based on terminal characteristics of individual inverters," *IEEE Transactions on Power Electronics*, pp. 1–1, 2015, doi: 10.1109/TPEL.2015.2483741.

[18] S. D. Panjaitan, R. Kurnianto, B. W. Sanjaya, and M. C. Turner, "Control of parallel inverters for high power quality and sharing accuracy in single-phase AC microgrids," in *2018 UKACC 12th International Conference on Control (CONTROL)*, Sep. 2018, pp. 50–55. doi: 10.1109/CONTROL.2018.8516761.

[19] X. Zou, X. Du, and G. Wang, "Modeling and stability analysis for multiple parallel grid-connected inverters system," in *2018 IEEE Applied Power Electronics Conference and Exposition (APEC)*, Mar. 2018, pp. 2431–2436. doi: 10.1109/APEC.2018.8341357.

[20] J. Yu, L. Deng, D. Song, and M. Pei, "Wide bandwidth control for multi-parallel grid-connected inverters with harmonic compensation," *Energies*, vol. 12, no. 3, p. 571, Feb. 2019, doi: 10.3390/en12030571.

[21] R. Ali and T. O'Donnell, "Analysis and mitigation of harmonic resonances in multi–parallel grid–connected inverters: a review," *Energies*, vol. 15, no. 15, p. 5438, Jul. 2022, doi: 10.3390/en15155438.

[22] W. Cao, K. Liu, S. Wang, H. Kang, D. Fan, and J. Zhao, "Harmonic stability analysis for multi-parallel inverter-based grid-connected renewable power system using global admittance," *Energies*, vol. 12, no. 14, p. 2687, Jul. 2019, doi: 10.3390/en12142687.

[23] X. Fu *et al.*, "A novel circulating current suppression for paralleled current source converter based on virtual impedance concept," *Energies*, vol. 15, no. 5, p. 1952, Mar. 2022, doi: 10.3390/en15051952.

[24] R. K. Gupta, V. M. Mishra, and N. K. Singh, "Elimination of circulating current in parallel operation of single phase inverter using droop controller," *Engineering Science and Technology, an International Journal*, vol. 28, 2022, doi: 10.1016/j.jestch.2021.06.005.

[25] H.-W. Choi and K.-B. Lee, "Review of methods for reducing circulating currents in parallel connected modular inverters," *Journal of Electrical Engineering & Technology*, vol. 18, no. 2, pp. 1227–1242, Mar. 2023, doi: 10.1007/s42835-023-01389-z.

[26] C. Qin, C. Zhang, A. Chen, X. Xing, and G. Zhang, "Circulating current suppression for parallel three-level inverters under unbalanced operating conditions," *IEEE Journal of Emerging and Selected Topics in Power Electronics*, vol. 7, no. 1, pp. 480–492, Mar. 2019, doi: 10.1109/JESTPE.2018.2813390.

[27] M. Aquib, A. S. Vijay, S. Doolla, and M. C. Chandorkar, "On circulating current mitigation for modular UPS/inverters," *IEEE Journal of Emerging and Selected Topics in Power Electronics*, vol. 11, no. 1, pp. 1179–1190, Feb. 2023, doi: 10.1109/JESTPE.2022.3187437.

[28] S. Suroso and H. Siswantoro, “Study of novel parallel H-bridge and common-emitter current-source inverters for photovoltaic power conversion system,” *International Journal of Power Electronics and Drive Systems (IJPEDS)*, vol. 13, no. 1, p. 500, Mar. 2022, doi: 10.11591/ijpeds.v13.i1.pp500-508.

[29] K. Kim, H. Cha, and H.-G. Kim, “A new single-phase switched-coupled-inductor DC–AC inverter for photovoltaic systems,” *IEEE Transactions on Power Electronics*, vol. 32, no. 7, pp. 5016–5022, Jul. 2017, doi: 10.1109/TPEL.2016.2606489.

[30] R. Panigrahi, S. K. Mishra, S. C. Srivastava, A. K. Srivastava, and N. N. Schulz, “Grid integration of small-scale photovoltaic systems in secondary distribution network—a review,” *IEEE Transactions on Industry Applications*, vol. 56, no. 3, pp. 3178–3195, May 2020, doi: 10.1109/TIA.2020.2979789.

[31] Suroso, Winasis, and T. Noguchi, “Overlap-time compensation technique for current-source power inverter,” *IET Power Electronics*, vol. 13, no. 4, pp. 854–862, Mar. 2020, doi: 10.1049/iet-pel.2019.0503.

[32] S. Suroso and T. Noguchi, “Multilevel current waveform generation using inductor cells and H-bridge current-source inverter,” *IEEE Transactions on Power Electronics*, vol. 27, no. 3, pp. 1090–1098, Mar. 2012, doi: 10.1109/TPEL.2010.2056933.

[33] F. Marignetti, R. L. Di Stefano, G. Rubino, and R. Giacomobono, “Current source inverter (CSI) power converters in photovoltaic systems: a comprehensive review of performance, control, and integration,” *Energies*, vol. 16, no. 21, p. 7319, Oct. 2023, doi: 10.3390/en16217319.

[34] A. Singh and B. Mirafzal, “An efficient grid-connected three-phase single-stage boost current source inverter,” *IEEE Power and Energy Technology Systems Journal*, vol. 6, no. 3, pp. 142–151, Sep. 2019, doi: 10.1109/JPETS.2019.2929952.

[35] V. Boscaino *et al.*, “Grid-connected photovoltaic inverters: Grid codes, topologies and control techniques,” *Renewable and Sustainable Energy Reviews*, vol. 189, p. 113903, Jan. 2024, doi: 10.1016/j.rser.2023.113903.

[36] H. Xiao, “Overview of transformerless photovoltaic grid-connected inverters,” *IEEE Transactions on Power Electronics*, vol. 36, no. 1, pp. 533–548, Jan. 2021, doi: 10.1109/TPEL.2020.3003721.

[37] J.-H. Lim, D.-I. Lee, Y.-J. Hyeon, and H.-S. Youn, “Differential power processing converter with active clamp structure and integrated planar transformer for power generation optimization of multiple photovoltaic submodules,” *IEEE Access*, vol. 11, pp. 5668–5678, 2023, doi: 10.1109/ACCESS.2023.3236675.

[38] B. K. Byford, L. E. Boucheron, B. H. King, and J. L. Braid, “Advanced photovoltaic module characterization: using image transformers for current–voltage curve prediction from electroluminescence images,” *IEEE Journal of Photovoltaics*, vol. 15, no. 4, pp. 557–565, Jul. 2025, doi: 10.1109/JPHOTOV.2025.3562931.

[39] S. Suroso, W. Winasis, and R. Supriyanti, “Study of parallel operation single phase H-bridge CSI and H-bridge VSI,” *International Journal of Power Electronics and Drive Systems (IJPEDS)*, vol. 16, no. 3, Sep. 2025, doi: 10.11591/ijpeds.v16.i3.pp1721-1730.

BIOGRAPHIES OF AUTHORS

Suroso received a B.Eng. degree in electrical engineering from Gadjah Mada University, Indonesia, in 2001, and an M.Eng. degree in electrical and electronics engineering from Nagaoka University of Technology, Japan in 2008. He was a research student at the Electrical Engineering Department, Tokyo University, Japan, from 2005-2006. He earned Ph.D. degree in the Energy and Environment Engineering Department, Nagaoka University of Technology, Japan, in 2011. He was a visiting researcher at the Electrical and Electronics Engineering Department, Shizuoka University, Japan, from 2009-2011. Currently, he is a professor at the Department of Electrical Engineering, Jenderal Soedirman University, Purwokerto, Central Java, Indonesia. His research interests include static power converters and their application in renewable energy conversion systems and electric vehicles. He can be contacted at email: suroso.te@unsoed.ac.id.

Winasis received a B.Eng. and M.Eng. from Gadjah Mada University, Indonesia. Currently, he is a lecturer in the Electrical Engineering Department, Jenderal Soedirman University. His research interests are power systems and renewable energy. He can be contacted at email: winasis@unsoed.ac.id.

Priswanto received a Master of Engineering from Gadjah Mada University, Indonesia. Currently, he is a lecturer in the Electrical Engineering Department, Jenderal Soedirman University. His research interests are control systems and renewable energy. He can be contacted at email: priswanto@unsoed.ac.id.